Metal Adlayer-Induced Relaxation of Au(111) Reconstruction under Electrochemical Control

Q. Wu, W. H. Shang, J. W. Yan, Z. X. Xie, and B. W. Mao*

State Key Laboratory for Physical Chemistry of Solid Surfaces, Chemistry Department, Xiamen University, Xiamen 361005, China

Received: November 13, 2002

Underpotential deposition of Sb has been observed to induce a relaxation of Au(111) ($\sqrt{3} \times 22$) reconstruction to corrugation lines of trigonal networks. The triangles typically appear pairwise with an average length of the baselines of ~20.2 ± 1.0 nm and a height of the triangles of ~10.6 ± 1.4 nm at a corrugation height of ~0.05 nm. The baselines of the trigonal network rotate by 30° with respect to the corresponding double rows of the ($\sqrt{3} \times 22$) reconstruction and align along one of the three {110} directions. An atomic resolution image reveals an apparent ($\sqrt{3} \times \sqrt{3}$) structure in the regions with hcp stacking sites enclosed by the triangles, which is attributed to the atomically dispersed surface alloy structure of Sb with the topmost Au atoms. Similar relaxation structures are observed with decreasing coverage via irreversible adsorption, although the size of the relaxation is alleviated. The surface alloying is confirmed by the creation of holes upon anodic stripping, the holes being confined at the connections between the two triangles. The results are rationalized as a consequence of compromise between two opposing effects: directional bonding via electron back donation, which tends to lift the reconstruction, and dislocation-mediated alloying, which favors the formation of relaxed reconstruction. The present study provides a good link with the studies in UHV as well as further knowledge for a thorough understanding of (sub)monolayer deposition in electrochemical environments.

Introduction

Clean surfaces of many transition and noble metals are reconstructed by rearranging atoms of the topmost layer with a higher density. The reconstruction is driven by an enhanced lateral attraction in the surface, which is created by the accumulation of extra charge density between surface atoms in response to the abrupt termination of the bulk crystal.[1,2] Accordingly, the stability of a clean reconstructed surface may be influenced by adsorption involving charge transfer to or from the substrate[1−3] and by surface charging in an electrolyte.[4−6] Detailed studies on this aspect have been carried out, focusing particularly on low-index Au single-crystal electrodes.[4] Surprisingly, however, as a major and unique category of adsorption, metal adatoms of submonolayer quantity via underpotential deposition (UPD[7,8]) in electrolytes seem to be missed in the topics relating to surface reconstruction. In the UPD process, metal atoms can be deposited at a potential that is positive with respect to the equilibrium potential of its bulk form because of stronger adatom−substrate binding energy than that of adatoms−adatoms. Strain is generally involved in the adlayer-covered surface because of the lattice mismatch. There also exists complexity due to possible adlayer−substrate alloying in the formation of the adlayer.[7] In many heteroepitaxial bimetallic or multicomponent systems that have a large lattice mismatch, reconstruction of the substrate or the prospective layer of a growing film has been observed to occur in UHV as a result of strain relief[9−11] or via strain-stabilized alloying.[12,13] It is anticipated that metal adlayers on electrode surfaces may influence the surface reconstruction in diverse ways.

In this paper, we report the Sb adlayer-induced transformation of Au(111) ($\sqrt{3} \times 22$) reconstruction in electrolytes. The Sb−Au system is distinct from many of the previously reported systems: With the sp^3-hybridization, Sb is a metal of directional bonding tendency, which may change the manner of adatom−substrate interaction; Sb and Au are miscible in the bulk in the form of $AuSb_2$[14] surface alloying being likely to take place in the surface layers at room temperature. These features could play an important role in the UPD process and stability of the reconstruction of the substrate surface. It is observed in this work that in the presence of the Sb adlayer the Au(111) ($\sqrt{3} \times 22$) reconstruction relaxes to corrugation lines of a trigonal network. The phenomenon is rationalized as a result of surface charge withdrawal via electron back donation of a substrate compromised by the dislocation-assisted alloying process.

* Corresponding author. E-mail: bwmao@xmu.edu.cn. Phone: +86 592 2186979. Fax: +86 592 2183047.

Experimental Section

In situ STM experiments were performed on a Nanoscope IIIa according to the established procedures.[15] A platinum wire was used as the quasi-reference electrode for in situ STM measurements, but potentials were quoted with respect to a saturated calomel electrode (SCE). Prior to each experiment, the working surface was subjected to electrochemical polishing and was blown dry by N_2. No flame annealing was applied.

Detailed studies of the general behavior of the Sb UPD and irreversible adsorption (IRA) have been reported elsewhere.[16,17] Briefly, the cyclic voltammogram of Au(111) in an Sb(III)-containing solution, as shown in Figure 1, gives two reduction peaks—D_1 (0.08 V) and D_2 (0.02 V)—corresponding to the electroreduction of the Sb(III) adspecies and the underpotential deposition of Sb from solution species, respectively. The charge flux associated with the UPD (D_2) and irreversible adsorption (IRA, D_1) is equivalent to coverages of $\theta_{Sb,upd} \approx 0.15$ ML and $\theta_{Sb,IRA} \approx 0.29$ ML, respectively. A steady cathodic residual current in a considerably wide potential range marked with D_3

10.1021/jp027459v CCC: $25.00
Published on Web 04/05/2003

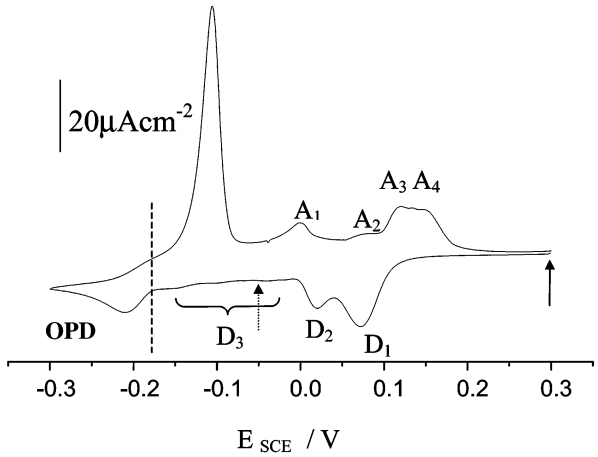

Figure 1. Cyclic voltammograms of Au(111) in 0.5 M H_2SO_4 solution containing saturated Sb_2O_3 (~1 mM Sb(III)) at a sweep rate of 5 mV s^{-1}. The arrows indicate the initial potential for the measurement (solid lines) and the potential (−0.05 V) at which dilute Sb(III) solution was introduced into the supporting electrolyte during in situ STM measurements to form an Sb UPD submonolayer (dashed lines).

arises from further deposition of small amounts of UPD Sb, whereas A_1 corresponds to its dissolution. Anodic peaks A_2 to A_4 are mixed features of UPD stripping associated with D_2 and the oxidation of Sb(0) back to Sb(III) associated with D_1.

Taking into account that the potential windows for surface reconstruction and for the UPD of many systems, including Sb on Au(111) of the present work, are often incompatible (the UPD often occurs at the potential prior to reaching a reconstructed surface), we introduced the Sb adlayer in the following way: At the potential of −0.05 V, where a stable reconstructed surface of clean Au(111) was ensured, a dilute oxygenated Sb(III)-containing solution was added at the midpoint of an in situ STM experiment without interrupting tip scanning, giving a final concentration of 0.1 mM for Sb(III) in the STM cell. Sb was electrochemically deposited as soon as the Sb(III) species diffused to the surface. Thus, irreversible adsorption could be avoided before UPD. A fixed amount of ~0.15 ML UPD Sb adlayer was thus obtained. For the purpose of introducing varying amounts of Sb adlayer at a fixed potential, the IRA approach was also adopted.[17] This was achieved by immersing the Au electrode in an Sb_2O_3-saturated (~1 mM Sb (III)) 0.5 M H_2SO_4 solution followed by subsequent reduction−oxidation cycling in the supporting electrolyte to obtain the desired amount of Sb.

Results and Discussions

Given in Figure 2a is the STM image of a clean reconstructed Au(111) surface in the supporting electrolyte of 0.5 M H_2SO_4 at −0.05 V. The characteristic double rows of the ($\sqrt{3} \times 22$) reconstruction run along one of the three {112} directions, which are indicated by lines numbered 1, 2, and 3, respectively. The double rows are as long as ~70 nm before bending at 120°. The image showing the (111) arrangement of atoms of the reconstructed Au surface is given as the inset of Figure 1a. Yet, the mesoscopic herringbone pattern that is frequently observed under UHV conditions[18] does not prevail under the present preparation conditions. Upon introducing a drop of Sb(III)-containing solution, the ($\sqrt{3} \times 22$) reconstruction was quickly removed, followed by the evolution of corrugation lines of trigonal arrangement over the entire surface (Figure 2b). The presence of dilute Sb(III) solution shifts the potential of the Pt quasi-reference electrode by ~30 mV in the negative direction, which would otherwise ensure the reconstructed surface. The transformation was complete within several minutes. Typically, triangles appear pairwise with an average length of the baselines of ~20.2 ± 1.0 nm and a height of the triangles of ~10.6 ± 1.4 nm. The height of the corrugation lines is ~0.05 nm, which is distinctively larger than that of 0.02 nm for the normal ($\sqrt{3} \times 22$) reconstruction.[18] The baselines of the trigonal network such as those indicated by lines numbered 1′, 2′, and 3′ in Figure 2b rotate by 30° with respect to the corresponding double rows of the normal reconstruction marked with 1, 2, and 3 in Figure 2a. Therefore, the baselines of the trigonal network align with one of the {110} direction. A close inspection to the triangles (Figure 2c−e) reveals that the corrugation lines are not even and smooth, which may well be a result of an accumulation of extra atoms of a certain kind. Atomic resolution imaging is extremely difficult. Nevertheless, Figure 2e gives the atomic resolution image for part of the surface in region A. A lattice of 3-fold symmetry in region A as well as on the corrugation lines is discerned with the nearest atomic distance of ~0.47 ± 0.03 nm. This value is close to the $\sqrt{3}$ distance of the (111) arrangement of an unreconstructed Au(111) surface. By comparison with the atomic distance of the ($\sqrt{3} \times 22$) reconstructed surface shown by the inset of Figure 2a, it is conceivable that the surface constituents are other than pure Au atoms. A similar procedure applied to unreconstructed Au(111) does not yield the trigonal network of corrugation lines.[17]

To examine the influence of Sb with different coverage, we performed additional measurements by introducing desired amount of Sb via IRA approach. With one or two potential cycling described in the Experimental Section, the fully covered Au(111) surface became partially exposed with a nonuniform distribution of Sb. This provides the surface with regions of different local coverage at a fixed potential although a quantitative determination of the coverage for each region is difficult. At −0.05 V, the irreversibly adsorbed Sb(III) is electroreduced to metallic Sb(0). The presence of a high coverage of Sb such as in region II or III of Figure 3a totally inhibited the normal reconstruction. Only in region I of Figure 3a, where the average coverage is estimated to be $\theta_{sb} \approx 0.1$ ML was there a tendency for the potential-induced reconstruction to build up at −0.08 V, as indicated by the arrows in the lower right corner of Figure 3a. A kinetically limited substantial rearrangement of surface atoms occurred over the entire terrace (Figure 3b). Eventually, similar corrugation lines of a trigonal network were created (Figure 3c). The vanishing of the Sb islands and the disorderliness of the surface morphology during the rearrangement clearly indicate the involvement of the alloying process. The subtle change in the step edges, as a result of the surface atom rearrangement, is also supportive of such an assumption.

In a separate experiment, a further decrease in coverage to $\theta_{sb} < 0.05$ ML (estimated from the image) can be obtained by applying more potential cycling to the irreversibly adsorbed Sb (Figure 4a). A typical potential-induced ($\sqrt{3} \times 22$) reconstruction easily built up at −0.08 V on such a surface (Figure 4b). The relaxation of the normal reconstruction occurred after resting at this potential for several minutes. A deformed herringbone structure rich in relaxed V-shaped elbows with a periodicity of ~10 nm was observed (Figure 4c). The small bright dots at the turning of the elbows are recognized as the Au islands squeezed out during alloying with the overlayer Sb. The results show that very little Sb could induce the transformation of the reconstruction, though the size of the relaxation is alleviated with decreasing coverage.

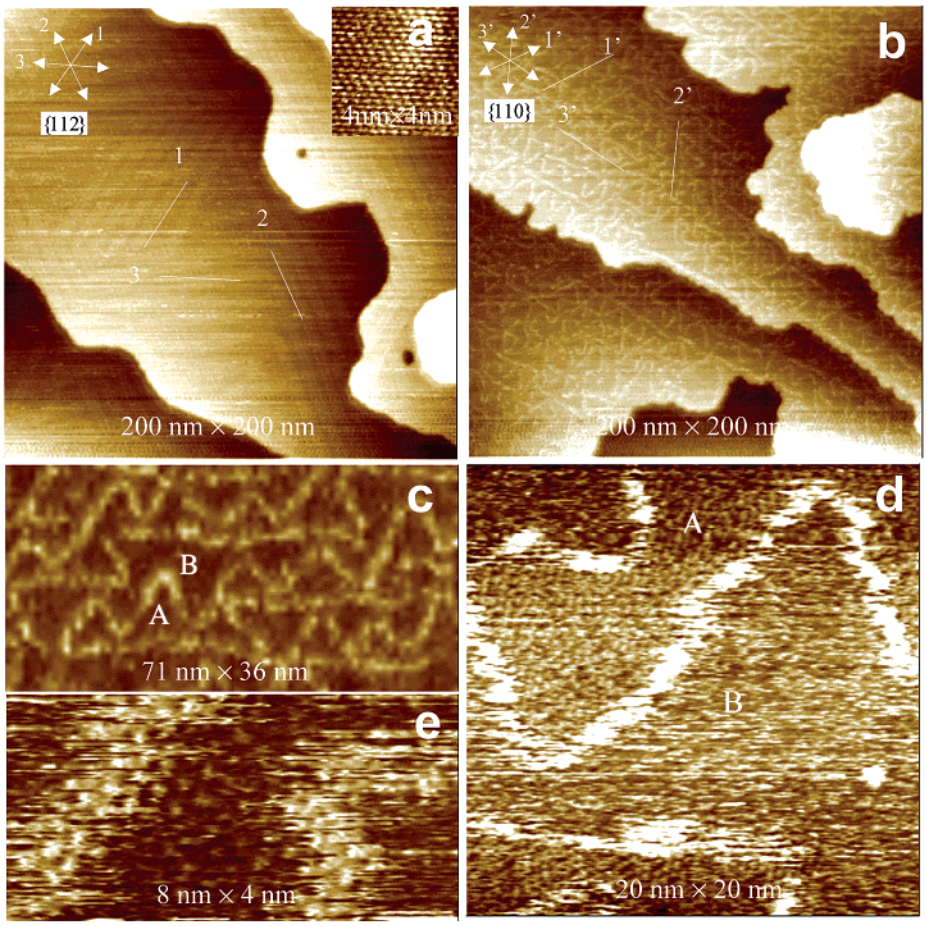

Figure 2. UPD Sb-induced relaxation of the Au(111) ($\sqrt{3} \times 22$) surface: (a) bare reconstructed Au(111) surface in 0.5 M H_2SO_4 at −0.05 V and (b) after the addition of dilute Sb(III) solution (b−e) at the same potential. The Sb adlayer with $\theta_{UPD,Sb} \approx 0.15$ ML relaxes the normal reconstruction into a trigonal network several minutes later. (c−e) Enlarged images of the trigonal network. The inset in (a) shows the atomic arrangement of the bare reconstructed Au(111) surface.

To verify the alloy involvement in the relaxation process, we examined the structural change in the trigonal network associated with anodic stripping. By very slow anodic potential sweeping (1 mV/s) to −0.03 V, the dealloying process is initiated by the generation of tiny, deep atomic holes at the connections of two triangles (Figure 5b). The dealloying rate increased with increased hole size at more positive potentials. The corrugation lines of the trigonal network were gradually removed during the process. Note that the IRA of Sb(III) took place upon increasing the potential, with flakes covering part of the surface (Figure 5d). From the confinement of the holes in that location, we propose a dislocation-mediated mechanism for the surface alloying and dealloying processes. It is noted that a further decrease in the potential would totally destroy the reconstruction, and large and deep holes (not shown) would be created upon anodic stripping at this stage, indicating severe alloying. This reveals that there is a critical negative potential and/or an upper limit of the amount of the Sb overlayer that restricts the alloying to within the topmost surface.

The trigonal corrugation lines of the present work closely resemble the V-shaped ridges of the Au(111)($\sqrt{3} \times 22$) reconstruction.[19] From the appearance of the pinched-off connections (~2 nm on average) of the two triangles, we identify the corrugation lines of the paired triangles to be the domain walls that separate regions of hcp (region A enclosed by the triangles) and fcc (region B outside the triangles) stacking sites of the substrate. Although the apparent height or corrugation in the STM image is influenced by the electronic effect, the ($\sqrt{3} \times \sqrt{3}$) structure in the hcp region (as well as on the corrugation lines) given in Figure 2e likely represents an atomically dispersed alloy of Sb and Au. This identification is corroborated with the extremely small size mismatch between Sb and Au atoms (<1%), which favors the incorporation of Sb into the Au surface lattice. With a much lower work function than that of Au, Sb manifests itself with a higher corrugation in the STM image in the shading of neighboring Au atoms to show the ($\sqrt{3} \times \sqrt{3}$) pattern. The possibility of the induced adsorption of SO_4^{-2} on Sb forming the ($\sqrt{3} \times \sqrt{3}$) pattern cannot be excluded, however, since Sb has a much more negative pzc than Au, which could induce anion adsorption on itself. In either case, Au atoms have to be expelled to accommodate the Sb atoms in the lattice. As a consequence, the uneven corrugation lines may well be due to the accumulation of extra Au atoms expelled during the intermixing process. This could also explain the larger corrugation height of the trigonal network. For Sb adsorption in region B, however, the energy cost for Sb incorporation into the surface lattice of this region must be sufficiently high, presumably because of the higher stability of the fcc stacking sites with lower energy. The adsorption of Sb adatoms in these regions appear to be mobile or floating over the surface, leading to severe scratching lines in the fcc region of the surface.

A domain model for the trigonal network is proposed on the basis of equilateral and paired triangles, as schematically shown in Figure 6. For simplicity, the model shows only part of the paired triangles, neglecting the ($\sqrt{3} \times \sqrt{3}$) arrangement on and

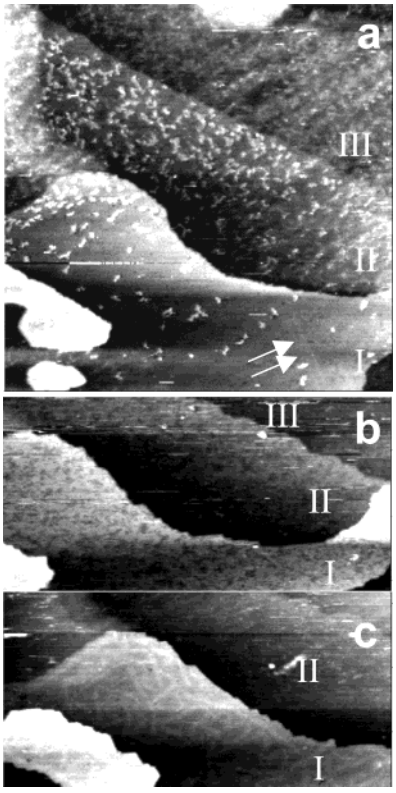

Figure 3. IRA Sb(0)-induced relaxation of the Au(111) reconstruction with $\theta_{IRA,Sb} \approx 0.1$ ML: (a) Sb(0)-covered Au(111) surface at -0.05 V, (b) substantial rearrangement of surface atoms in region I ($\theta_{IRA,Sb} \approx 0.1$ ML) at -0.08 V, and (c) emergence of the trigonal network of corrugation lines 20 min later. Solution: 0.5 M H_2SO_4. Scan size: (a) 130 nm × 130 nm, (b, c) 130 nm × 65 nm.

unsmoothness of the corrugation lines. The atoms at the corrugation lines occupy the bridge sites and separate the hcp and fcc stacking sites. Two extra columns of atoms along two of the three sides in each triangle can be accommodated for the transition from fcc to hcp stacking sites, which is equivalent to an ~3.8% compression with respect to the normal (111) arrangement for an equilateral triangle with side lengths of ~10 nm. In the hcp region, Sb intermixes with Au in a $(\sqrt{3} \times \sqrt{3})$ registration, which is equivalent to a fractional coverage of 0.33 ML for Sb in this region. Neglecting Sb adsorption in the fcc region outside the triangles would give an average Sb coverage of ~0.16 ML over the surface. This value is in agreement with the coverage of $\theta_{UPD\ Sb} \approx 0.15$ ML that is estimated on the basis of the charge flux for deposition on a cyclic voltammogram. For comparison, the normal $(\sqrt{3} \times 22)$ reconstruction with a uniaxial compression of ~ 4.4% of surface atoms along the $[1\bar{1}0]$ directions is also schematically shown as the inset of Figure 6.

Our experimental results can be rationalized as a consequence of compromise between two opposing effects: the directional bonding via electron back donation, which tends to lift off of the reconstruction, and the dislocation-mediated alloying, which favors the formation of a relaxed reconstruction that is rich in elbows. It is well known that Sb has a valence electron configuration of $4d^{10}5s^25p^3$ with a very low energy level of the empty 5d orbital.[20] Although Sb is less electronegative, it is likely that upon adsorption Sb receives back-electron donation from Au by filling the empty d orbital of Sb to form a bond with directionality of a certain extent, making itself virtually an electron withdrawer. A direct consequence of the surface charge reduction would be the tendency toward the lifting of the reconstruction. This tendency, however, is rendered by the alloy formation, which is mediated by the dislocation formation. It is known that the elbows of the herringbone pattern in the Au(111) $(\sqrt{3} \times 22)$ reconstruction contain stacking dislocations that are of higher energy than those of the fcc and hcp sites. We expect that the turnings of the corrugation lines of the trigonal network are also of the highest energy among other stacking sites and that the alloying−dealloying process would be more favorable via these higher-energy dislocations. The dilution of the Au surface atoms in the hcp stacking sites by the incorporation of Sb atoms alleviates the compression of surface atoms by forming the mesoscopic trigonal network of domain walls. Therefore, the energy cost in forming the dislocation must be overcome by the energy gain in forming the atomically dispersed surface alloy.

Similar trigonal networks of 3-fold symmetry were reported previously in the UHV environment on the alkali-covered Au(111) surface[3] as well as in heteroepitaxial bimetallic[9,10] or multicomponent[11,13] systems that have a large size misfit. For the alkali-covered Au(111) surface, the effect is interpreted as an adsorbate-induced weakening of the coupling between the first two Au layers. In view of the influence of the overlayer on the surface reconstruction, our system of Sb on Au(111) contrasts with the alkali-covered Au(111) system: the alkali metal induces the relaxed reconstruction whereas Sb relaxes the normal reconstruction. This contrast is assumed to originate from the different nature of the adsorbates: alkali metals donate charge to the substrate Au surface whereas Sb withdraws charge from the substrate. Our results are very similar to the alloying-driven reconstruction observed in the co-deposition of thin Ag and Cu films on Ru(0001).[11] This multicomponent system has a large lattice mismatch. The formation of the trigonal network

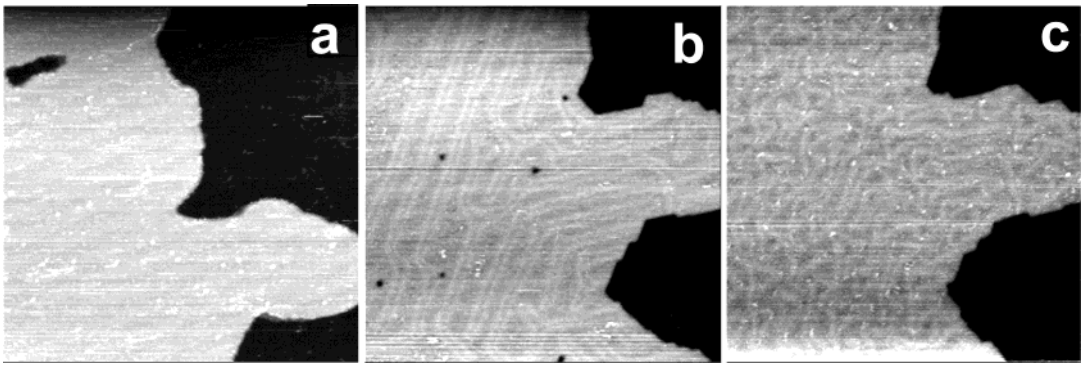

Figure 4. IRA Sb(0)-induced relaxation of the Au(111) reconstruction with $\theta_{IRA,Sb} < 0.05$ ML: (a) Sb(0)-covered Au(111) surface at -0.05 V, (b) build up of the normal $(\sqrt{3} \times 22)$ reconstruction at -0.08 V, (c) transformation into a distorted reconstruction structure rich in dislocations 16 min after b. Scan size: 100 nm × 100 nm. Solution: 0.5 M H_2SO_4.

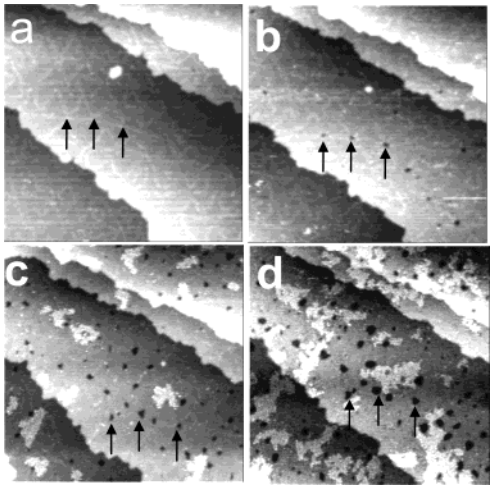

Figure 5. Anodic stripping of Sb from a relaxed Au(111) surface: UPD Sb-induced relaxation of the Au(111) ($\sqrt{3} \times 22$) surface prior to stripping at (a) −0.04 V and various stages during anodic stripping at (b) −0.03 V, (c) − 0.02 V, and (d) 0.1 V. Holes are generated and confined at the connections of two triangles though the size of the holes increases upon increasing potential from b to d. The white flakes covering the surface in c and d are due to the IRA of Sb(III) from the solution. Solution: 0.5 M H_2SO_4 + 0.05 mM Sb(III). Scan size: 100 nm × 100 nm.

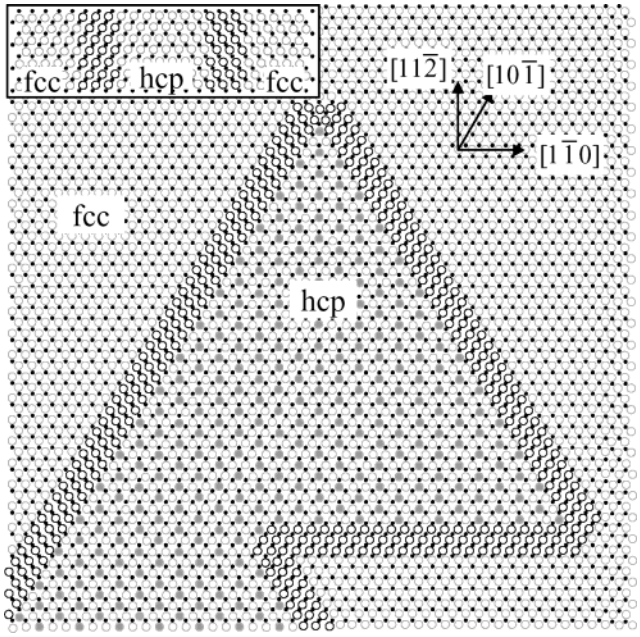

Figure 6. Model for the Sb adlayer-induced trigonal networks of corrugation lines. Black dots: second layer atoms of Au. Gray circles: fcc and hcp-type topmost Au atoms. Dark circles: bridge-type topmost Au atoms. Gray filled circles in the hcp region: Sb atoms incorporated into the Au surface lattice plane. The model for normal ($\sqrt{3} \times 22$) reconstruction prior to relaxation is given as the inset in the upper left corner, which shares the same notation for atoms and lattice directions.

of domain walls is a result of strain relaxation upon alloying mediated by Ru atoms of the substrate. In our system, strain due to the adsorption of Sb would be neglectfully small and cannot account for the observed relaxation phenomenon of the system. It is known that transition and noble metals typically have tensile stress whereas surfaces of substances with directional dangling bonds have compressive stress.[1,2] Stresses of opposite signs (tensile for Au and compressive for Sb) could have played a dominant role in the atomically dispersed alloying and relaxation of the reconstruction in the present work.

Conclusions

In summary, we have observed the relaxation of Au(111) reconstruction induced by a submonolayer of electrodeposited Sb. To the best of our knowledge, this is the first example of the adlayer effect on the surface reconstruction in electrolytes. It should be distinguished from the anisotropy of the metal adlayer structures observed in the UPD of submonolayers Cd[21] and Sn[15] on Au(111) a result of interference from the substrate anisotropy. Combining the results from both kinds of the systems, however, proves the close interplay between the metal adlayer and the reconstructed Au(111) surface. The adlayer-induced relaxation phenomenon in electrolytes is expected to be important because it provides not only a good complement to the related studies in UHV but also further knowledge for a thorough understanding of (sub)monolayer deposition in electrochemical environments.

Acknowledgment. We gratefully acknowledge financial support from the Natural Science Foundation of China (NSFC nos. 29973040, 29833060, and 20021002) and valuable discussions with Dr. X. Lu and Dr. D. Y. Wu.

Supporting Information Available: Explanation of the cleanness of a Au(111) surface without flame annealing and related data. More detailed description for introducing IRA Sb. More STM images showing the dynamics of the relaxation and the transition of IRA Sb(III) to metallic Sb(0). This material is available free of charge via the Internet at http://pubs.acs.org.

References and Notes

(1) Ibach, H. *Surf. Sci. Rep.* **1997**, *29*, 193.
(2) Haiss, W. *Rep. Prog. Phys.* **2001**, *64*, 591.
(3) Barth, J. V.; Behm, R. J.; Ertl, G. *Surf. Sci. Lett.* **1994**, *302*, L319. Barth, J. V.; Behm, R. J.; Ertl, G. *Surf. Sci.* **1995**, *341*, 62.
(4) Lipkowski, J.; Shi, Z.; Chen, A.; Pettinger, B.; Bilger, C. *Electrochim. Acta* **1998**, *43*, 2857.
(5) Kolb, D. M. Prog. *Surf. Sci.* **1996**, *51*, 109. Dakkouri, A. S.; Kolb, D. M. In *Interfacial Electrochemistry*; Wiecowski, A., Ed.; Marcel Dekker: New York, 1999.
(6) Heine, V.; Marks, L. D. *Surf. Sci.* **1986,** *165*, 65.
(7) Kolb, D. M. In *Advances in Electrochemistry and Electrochemical Engineering*; Gerischer, H., Tobias, Ch. W., Eds.; Wiley: New York, 1978; Vol. 11, p 125.
(8) Herrero, E.; Buller, L. J.; Abrunã, H. D. *Chem. Rev.* **2001**, *101*, 1897 and references therein.
(9) Holst, B.; Nohlen, M.; Wandelt, K.; Allison, W. *Phys. Rev. B* **1998**, *58*, R1095.
(10) Gunther, C.; Vrijmoeth, J.; Hwang, R. Q.; Behm, B. J. *Phys. Rev. Lett.* **1995**, *74*, 754.
(11) Steven, J. L.; Hwang, R. O. *Phys. Rev. Lett.* **1995**, *74*, 2078.
(12) Thayer, G. E.; Ozolins, V.; Schmid, A. K.; Bartelt, N. C.; Asta, M.; Hoyt, J. J.; Chinag, S.; Hwang, R. W. *Phys. Rev. Lett.* **2001**, *86*, 660.
(13) Stevens, J. L.; Hwang, R. W. *Phys. Rev. Lett.* **1995**, *74*, 2078.
(14) Simić, V._Marinković, Z. *J. Mater. Sci.* **1998**, *33*, 561.
(15) Mao, B. W.; Tang, J.; Randler, R. *Langmuir* **2002**, *18*, 5329.
(16) Jung, G.; Rhee, C. K. *J. Electroanal. Chem.* **1997**, *436*, 277.
(17) Wu, Q.; Shang, W. H.; Yan, J. W.; Mao, B. W. *J. Mol. Catal.* In press.
(18) Barth, J. V.; Brune, H.; Ertl, G.; Behm, R. J. *Phys. Rev. B* **1990**, *42*, 9307.
(19) Narasimhan, S.; Vanderbilt, D. *Phys. Rev. Lett.* **1992**, *69*, 1564.
(20) Cotton, F. A. *Advanced Inorganic Chemistry*; Wiley & Sons: New York, 1972.
(21) Bondos, J. C.; Andrew, A. G.; Nuzzo, R. G. *J. Phys. Chem.* **1996**, *100*, 8671.